Pumping wavelength related population inversion in Nd:doped laser

YINGXIN BAI

Affiliations
NASA Goddard Space Flight Center, Code 554, Greenbelt, MD 20771.
Email: yingxin.bai-1@nasa.gov

ABSTRACT

Pumping wavelength related population inversion in Nd:doped laser has been investigated, where the laser is regarded as two thermodynamic equilibrium systems, upper state one and lower state one. The population inversion limits at various pumping wavelengths and temperatures are compared. The effective metastable life time has been derived, where both pump and laser fields within Nd:doped laser medium reduce the lifetime. The saturation of lifetime is discussed. As a result, in-band pumping of Nd: doped laser is good for improving the efficiency and achieving narrow-linewidth of laser wavelength due to less population inversion; off-band pumping is benefit for extracting high pulse energy thanks of large population inversion.

Diode-pumped solid-state lasers (DPSSLs) with the advantages in compactness and efficiency have been widely investigated. Nd:YVO_4 and Nd:$GdVO_4$ laser crystals have several spectroscopic properties, such as large, stimulated emission cross section and strong broadband absorption around 808 nm that are particularly relevant to AlGaAs laser diode pumping. However, they suffer from poor thermomechanical properties resulting in beam degradation and crystal fracture. In-band pumping with 880/888/914 nm laser diodes is helpful to reduce quantum defect, enhance the laser efficiency, and mitigate thermal effects of Nd:YVO_4/$GdVO_4$ lasers.

In 1963, a diode-pumped solid-state laser was first investigated where a Nd:$CaWO_4$ laser was directly in-band pumped into the $^4F_{3/2}$ upper level by 880 nm radiation of GaAs diodes.[1] Later, the in-band pumping research was focused on Yb:doped laser, Er:doped laser, and Ho:doped laser because of their energy level structures.[2-5] High power and high efficiency diode-pumped thin-disk Yb:YAG laser and Yb:doped fiber laser have been developed.[6,7] In recent years, great attention has been paid to in-band pumped Nd:doped laser again because high power AlGaAs laser diodes can also operate in the wavelength of 880/888nm.[8] For example, in-band pumped Nd:YAG nonplanar ring oscillator (NPRO) has been demonstrated in high efficiency and power.[9] The developed high power InGaAs laser diodes in the research of diode pumped Yb:doped lasers at the wavelength of 914 nm can also be used as the pump sources of Nd:YVO_4/$GdVO_4$ lasers . The commercially available 914 nm InGaAs laser diodes have even higher efficiency than 880 nm AlGaAs laser diodes. Experimentally, the 80.7% slope efficiency and 78.7% optical-to-optical efficiency have been achieved in a 914 nm diode pumped continuous wave (CW) Nd:YVO_4 laser with an M^2=1.1 beam quality.[10] The slope efficiency is near the quantum limited efficiency (914/1064 ≈85.9%). In contrast, the slope efficiency of 808 nm diode pumped CW Nd:YVO_4 laser is about 58%, far-off the quantum limited efficiency (808/1064≈75.9%). In-band directly pumped Nd:doped laser evades non-radiation relaxation between pump and laser upper manifolds like the reduction of internal resistance in an electrical circuit. It speeds up the energy transfer between pump and laser (the non-radiation relax time of off-band pumping is approximately in an order of nanosecond order), and eliminates the ions upper state leaking (the pump and laser in off-band pumping have their respective upper states, and undergoes a large upper state ions leaking). It also increases the lifetime of laser upper state (small heat loading results in low crystal temperature) and reduces the saturation effect (the saturation intensity of in-band direct pumping is larger than that of off-band indirect pumping).

Now, people no longer believe that the 4-level operation, which is well suited for flash-lamp pumped Nd:doped laser, is the best choice for diode pumped Nd:doped laser. Many applications, like active remote sensing, need Q-switched lasers to generate high energy laser pulses. The improvement in in-band pumped Q-switched Nd:doped laser is still going on. A suitable theoretical model is needed for analysis, simulation, and approach election. For example, all-solid-state laser transmitters for sodium lidar and guide star may be developed based on Q-switched Nd:doped lasers One approach is the sum frequency generation of 1064 nm and 1319 nm Nd:YAG laser pulses; the other is the second harmonic generation of 1066 nm Nd:YVO_4 pumped mixed $Gd_xY_{1-x}VO_4$ Raman laser pulses at the wavelength of 1178 nm. Raman approach seems to be compact and efficient.[11] Experimentally, the improvement of in-band pumped Nd:YVO_4 laser, especially in low repletion rate and high pulse energy mode, was not successful.[12] An empirical analysis was attributed to "…that fluorescence quenching and up-conversion processes limit the possible uses for the 914 nm pumping scheme to regimes with low population inversions."

In this letter, the physics analysis of lowering the limitation of population inversion is presented based on the Boltzmann probability

distribution of energy levels. Fig.1 shows the energy level diagram of Nd:YVO_4 crystal. For 808 nm pumping wavelength, the Nd:YVO_4 laser is a 4-level system; for 880/888/914 nm diode pumping wavelength, the Nd:YVO_4 laser is regarded as a quasi-3-level system, referred to as a Λ-shaped 3-level system because the pump and laser share the same upper state

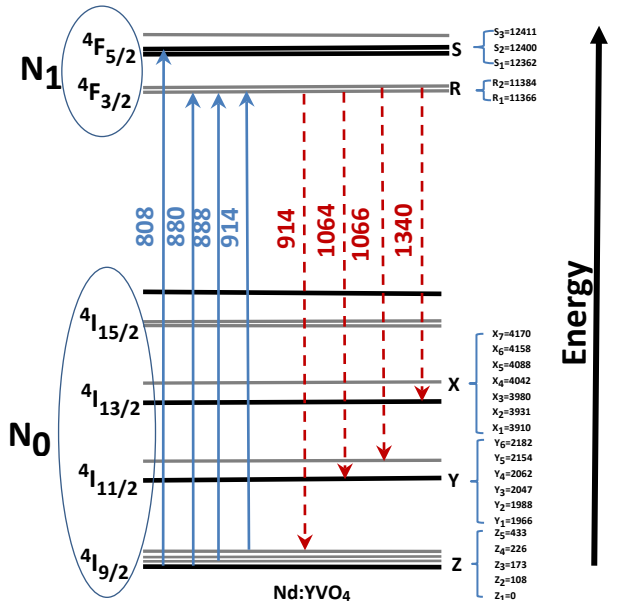

Fig. 1. Energy level diagram of Nd^{+3} ions doped YVO_4 crystal. The data of energy sublevels are from Ref. 13.

In a 4-level system, the pump and laser upper states are assumed in a thermal equilibrium system because the non-radiative relaxation time between the manifolds $^4F_{5/2}$ and $^4F_{3/2}$ could be ignored compared to the lifetime of the metastable energy manifold $^4F_{3/2}$. N_1 denotes the population density of Nd^{3+} ions in this thermal equilibrium system. By analogue, the pump and laser lower states are assumed in other thermal equilibrium system where the population density of Nd^{3+} ions is noted as N_0. The total population density of Nd^{3+} ions is $N_T = N_1 + N_0$. Regardless of whether it is a 4- or 3-level system, it will be simplified into two thermal equilibrium systems: the upper state one and the lower state one. In each thermal equilibrium system, the population density can be described by Boltzmann probability distribution:

$$f_i = \frac{g_i e^{-\varepsilon_i/kT}}{\sum_{j=1}^{M} g_j e^{-\varepsilon_j/kT}} \quad (1)$$

where f_i, g_i, and ε_i are the probability population density, the degeneracy factors, and the energy of level i, respectively, k is the Boltzmann constant, T is the thermodynamic temperature of the system, and M is the total number of all levels in the interested thermal equilibrium system, either N_1 or N_0. In the interested thermal equilibrium systems, all degeneracy factors are 1. The pump and laser are varying the magnitudes of N_1 and N_0, but they don't influence the total population density N_T (constant).

In a Λ-shaped 3-level system, the transition between R_1 (the lowest sublevel in manifold of $^4F_{3/2}$) and Z_5 (the highest sublevel in manifold of $^4I_{9/2}$) corresponds to the laser wavelength of 914 nm. Without population inversion, 914 nm laser is absorbed so that the population in the manifold of $^4I_{9/2}$ is increasing. With population inversion, 914 nm laser is amplified, so that the population in manifold of $^4I_{9/2}$ is decreasing.[14]. It is impossible for 914 nm pump laser to make the population inversion between R_1 and Z_5 sublevels. On the other word, the maximum contribution of 914 nm pump laser is to make the population in R_1 sublevel equal to the population in Z_5, that is

$$N_{Z_5} = N_{R_1}, \quad (2)$$

where the population in Z_5 sublevel of $^4I_{9/2}$ manifold (lower state) and the population in R_1 sublevel of $^4F_{3/2}$ manifold (upper state) are written as, respectively,

$$N_{Z_5} = f_{Z_5} N_0, \quad (3)$$

$$N_{R_1} = f_{R_1} N_1. \quad (4)$$

Assuming the temperature $T = 300\,K$ (just above the room temperature), $f_{Z_5} = 5.02\%$ and $f_{R_1} = 51.56\%$. In respect to the total population density, $N_T = N_1 + N_0$, the probability distribution of population in R_1 sublevel can be defined as

$$f_{R_1}^{(T)} = \frac{N_{R_1}}{N_T}. \quad (5)$$

For an extreme pumping intensity ($N_{Z_5} = N_{R_1}$),

$$\frac{1}{f_{R_1}^{(T)}} = \frac{1}{f_{Z_5}} + \frac{1}{f_{R_1}}. \quad (6)$$

Therefore, the limitation of population in R_1 sublevel is $f_{R_1}^{(T)} = 4.58\%$ when a Nd:YVO_4 crystal is pumped by 914 nm diode and at the temperature of $T = 300\,K$. Similarly, the probability distribution of population in R_2 sublevel can be defined as

$$f_{R_2}^{(T)} = \frac{N_{R_2}}{N_T}. \quad (7)$$

The ratio between populations in R_2 and R_1 sublevels within the manifold of $^4F_{3/2}$ can be calculated by Boltzmann factor,

$$\frac{f_{R_2}}{f_{R_1}} = e^{-\frac{\varepsilon_{R_2} - \varepsilon_{R_1}}{kT}}, \quad (8)$$

where $$N_{R_2} = f_{R_2} N_1. \quad (9)$$

At the temperature of $T = 300\,K$, the ratio $f_{R_2}/f_{R_1} = 0.9173$ and $f_{R_2}^{(T)} = (f_{R_2}/f_{R_1})\, f_{R_1}^{(T)} = 4.20\%$. Fig. 2 shows that the population in the manifold of $^4F_{3/2}$ (sum of maximum populations in R_1 and R_2) is 8.78%. If the manifold of $^4I_{11/2}$ is empty, 8.78% is the population inversion limitation of 1064, 1066, or 1340 nm laser. In the same way, the population inversion limitations to other diode pumping wavelengths are 31.40% for 888 nm and 43.45% for 880 nm.

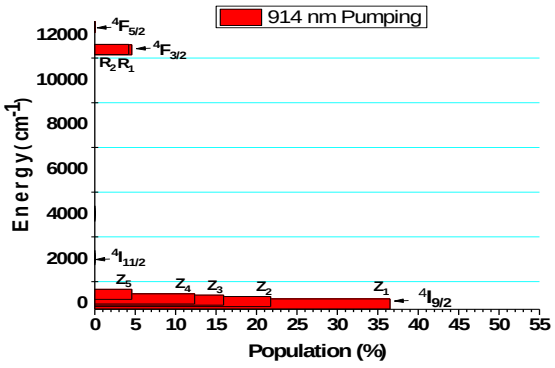

Fig. 2. The population distribution of Nd^{3+} doped YVO_4 crystal at the temperature of 300 K when an extreme pumping intensity at wavelength of 914 nm is applied.

A 808 nm diode pumped Nd:YVO_4 laser is a 4-level system. For 1064 nm laser wavelength, the thermal equivalence ratio of pump upper state (S_2 sublevel of $^4F_{5/2}$ manifold) to laser upper state (Y_1 sublevel of $^4I_{11/2}$ manifold) can be also described by Boltzmann factor,

$$\frac{f_{pu}}{f_{lu}} = e^{-\frac{\varepsilon_{pu}-\varepsilon_{lu}}{kT}}, \qquad (10)$$

where f_{pu} and f_{lu} are the probabilities of pump and laser upper states; ε_{pu} and ε_{lu} are the energy levels of pump and laser upper states. For a 808 nm diode pumped 1064 nm Nd:YVO_4 laser, the ratio is 1/142. At the maximum of population inversion, the population on the pump upper state (S_2 sublevel of $^4F_{5/2}$ manifold) is equal to the population on pump lower state (Z_1 sublevel of $^4I_{9/2}$ manifold), that is, 51.11%, as shown in Fig. 3. The calculated population inversion limitation for 808 nm pumping is 97.99%. In brief, the population inversion limitation is not an issue for a 4-level laser system, while for a Λ-shaped 3-level system, especially a high energy laser with a low repetition rate, it should be carefully well-thought-out.

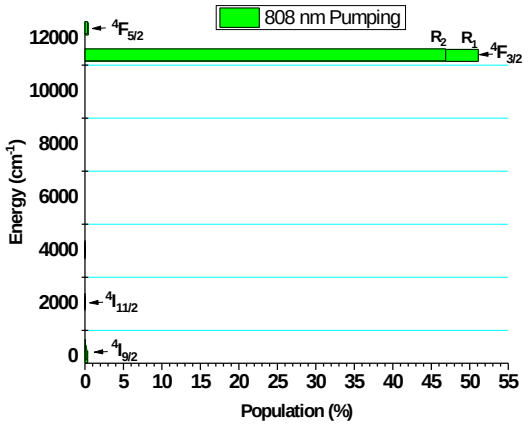

Fig. 3. The population distribution of Nd^{3+} doped YVO_4 crystal at the temperature of 300 K when an extreme pumping intensity at wavelength of 808 nm is applied

We can calculate a population inversion limitation of 1064 nm for different pump wavelengths at various temperatures. Table 1 lists the mentioned-above wavelengths associated with population inversion limitations for 1064, 1066, or 1340 nm Nd:YVO_4 laser at the temperature of 300 K and 400 K. For 914 nm pumping, the population inversion limitation is increasing with temperature (from 300 K to 400 K), for 808, 880, or 888 nm pumping, it is decreasing.

Table 1. Pump wavelength-dependent population inversion limitations

Pump Wavelength (nm)		808	880	888	914
Max. Population (%) T=300 K	R_1	51.11	22.66	16.38	4.58
	R_2	46.87	20.79	15.02	4.20
Population Inversion Limit (%) T=300K	$^4F_{3/2}$	97.99	43.45	31.40	8.78
Max. Population (%) T=400 K	R_1	48.02	20.88	16.20	6.42
	R_2	45.01	19.15	15.18	6.02
Population Inversion Limit (%) T=400K	$^4F_{3/2}$	93.03	40.03	31.38	12.44

The population inversion is directly proportional to the small signal gain of pulse amplification. The population inversion limitation implies the energy extraction under extremal pumping. At a temperature of 300 K, the maximum population inversion of Nd:YVO_4 laser pumped by 914 nm diode is only 9% of that pumped by 808 nm diode; and at 400 K, the population inversion limitation of 808 nm diode pumped Nd:YVO_4 laser is approximately 7.5 time higher than that of 914 nm diode pumped one. This model can clearly and unambiguously interpret the experimental results, where the gain of 808 nm diode pumped laser is 5 times higher than that of the 914 nm pumped laser when 12 W pump power is absorbed.

For the detail analysis, the temperature distribution within the crystal should be carefully considered. The higher the power absorbed by Nd:YVO_4 crystal, the higher the crystal temperature, and the closer it is to the population inversion limitation.

For the sake of general-utility, Fig.4 shows the energy-level diagram of a 4–level system like a Nd:doped laser pumped by 808 nm laser diode, where the levels **d** and **b** are the upper states of pump and laser, and the levels **a** and **c** are the lower states of pump and laser, respectively. If the levels **d** and **b** merge together, the system will become a Λ-shaped 3-level system like a Nd:doped laser pumped by 880, 888, or 914 nm laser diode

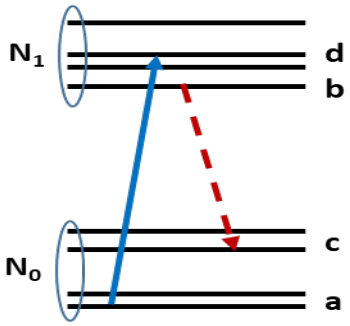

Fig. 4. The diagram of pump and laser transitions in a 4-level system.

For a 4-level system, the coupled differential equations between pump and laser can be written as

$$\frac{dN_1}{dt} = \sigma_{ab}\left(\frac{N_a}{g_a} - \frac{N_d}{g_d}\right)\phi_P - \sigma_{em}\left(\frac{N_b}{g_b} - \frac{N_c}{g_c}\right)\phi_L - \frac{N_1}{\tau_0}, \qquad (11)$$

$$\frac{d\phi_P}{dz} = -\sigma_{ab}\left(\frac{N_a}{g_a} - \frac{N_d}{g_d}\right)\phi_P, \qquad (12)$$

$$\frac{d\phi_L}{dz} = \sigma_{em}\left(\frac{N_b}{g_b} - \frac{N_c}{g_c}\right)\phi_L, \qquad (13)$$

where $N_a = f_a N_0$, $N_b = f_b N_1$, $N_c = f_c N_0$, $N_d = f_d N_1$, σ_{ab} and σ_{em} are the individual absorption and emission cross sections, τ_0 is the fluorescence lifetime of upper manifold, ϕ_P and ϕ_L are the pump and laser photon flux densities in the crystal. z and t are the propagating distance and time of pump/laser beams within the laser crystal. For the steady-state operation ($dN_1/dt = 0$), the solutions of Eq. (11) will be

$$N_1 = \frac{\sigma_{ab}\frac{f_a}{g_a}\phi_P + \sigma_{em}\frac{f_c}{g_c}\phi_L}{\sigma_{ab}\left(\frac{f_a}{g_a}+\frac{f_d}{g_d}\right)\phi_P + \sigma_{em}\left(\frac{f_b}{g_b}+\frac{f_c}{g_c}\right)\phi_L + \frac{1}{\tau_0}} N_T, \qquad (14)$$

$$N_0 = \frac{\sigma_{ab}\frac{f_d}{g_d}\phi_P + \sigma_{em}\frac{f_b}{g_b}\phi_L + \frac{1}{\tau_0}}{\sigma_{ab}\left(\frac{f_a}{g_a}+\frac{f_d}{g_d}\right)\phi_P + \sigma_{em}\left(\frac{f_b}{g_b}+\frac{f_c}{g_c}\right)\phi_L + \frac{1}{\tau_0}} N_T. \qquad (15)$$

Briefly, the upper/lower state populations depend on the photon flux densities of pump and laser as well as the lifetime of metastable state. The effective metastable state lifetime τ_e satisfies following equation

$$\frac{1}{\tau_e} = \sigma_{ab}\left(\frac{f_a}{g_a} + \frac{f_d}{g_d}\right)\phi_P + \sigma_{em}\left(\frac{f_b}{g_b} + \frac{f_c}{g_c}\right)\phi_L + \frac{1}{\tau_0}. \quad (16)$$

Later, the saturation of metastable state lifetime will be discussed.

Generally, the laser amplification is presented as

$$\frac{dI_L}{I_L dz} = \frac{g}{1+\frac{I_L}{I_{LS}}}, \quad (17)$$

where $I_L = \phi_L h\nu_L$, g and I_{LS} are the small signal gain coefficient and the saturation intensity, and h and ν_L are Planck constant and laser frequency, respectively. Inserting Eqs. (14) and (15) into Eq. (13) and then comparing with Eq. (17), the corresponding small-signal gain coefficient and the saturation intensity can be obtained,

$$g(\phi_P) = \frac{\sigma_{ab}\phi_P\tau_0\left(\frac{f_a f_b}{g_a g_b} - \frac{f_c f_d}{g_c g_d}\right) - \frac{f_c}{g_c}}{\sigma_{ab}\phi_P\tau_0\left(\frac{f_a}{g_a} + \frac{f_d}{g_d}\right)+1}\sigma_{em}N_T, \quad (18)$$

$$I_{LS}(\phi_P) = \frac{\sigma_{ab}\phi_P\tau_0\left(\frac{f_a}{g_a} + \frac{f_d}{g_d}\right)+1}{\sigma_{em}\tau_0\left(\frac{f_b}{g_b} + \frac{f_c}{g_c}\right)}h\nu_L. \quad (19)$$

Both are functions of pumping intensity. Without pumping, $g(0) = -\sigma_{em}\left(\frac{f_c}{g_c}\right)N_T$, where σ_{em} corresponds to the measured absorption cross section at the laser wavelength.

Analogously, the pump absorption and saturation can be discussed:

$$\frac{dI_P}{I_P dz} = -\frac{\alpha}{1+\frac{I_P}{I_{PS}}}, \quad (20)$$

Where

$$\alpha(\phi_L) = \frac{\sigma_{em}\phi_L\tau_0\left(\frac{f_a f_b}{g_a g_b} - \frac{f_c f_d}{g_c g_d}\right) + \frac{f_a}{g_a}}{\sigma_{em}\phi_L\tau_0\left(\frac{f_b}{g_b} + \frac{f_c}{g_c}\right)+1}\sigma_{ab}N_T, \quad (21)$$

$$I_{PS}(\phi_L) = \frac{\sigma_{em}\phi_L\tau_0\left(\frac{f_b}{g_b} + \frac{f_c}{g_c}\right)+1}{\sigma_{ab}\tau_0\left(\frac{f_a}{g_a} + \frac{f_d}{g_d}\right)}h\nu_P. \quad (22)$$

They are the functions of laser intensity. Without lasing, $\alpha(0) = \sigma_{ab}\left(\frac{f_a}{g_a}\right)N_T$, where σ_{ab} is the absorption cross section at the pump wavelength. For the detail description of CW operation, the non-radiation relaxation within the upper state or lower state thermodynamic equilibrium system should be counted even though these relax times might be in the order of nanosecond. For a simple modification, different upper-manifold fluorescence lifetimes should be applied for in-band direct pumping and off-band indirect pumping because the relaxation between pump and laser upper manifolds causes the time delay.

For Q-switching operation, the time delay caused by the relaxation between pump and laser upper manifolds might be ignored, and the laser intensity is zero during pumping. If pump intensity is fixed, the solution of Eq. (11) can be rewritten as

$$N_1 = \alpha(0)\phi_P\tau\left(1 - e^{-t/\tau}\right), \quad (23)$$

where

$$\tau = \frac{\tau_0}{1+\frac{I_P}{I_{PS(0)}}}, \quad (24)$$

$$I_P = \phi_P h\nu_P, \quad (25)$$

$$I_{PS}(0) = h\nu_P \Big/ \left[\sigma_{ab}\tau_0\left(\frac{f_a}{g_a} + \frac{f_d}{g_d}\right)\right]. \quad (26)$$

Using $\frac{f_b}{g_b}$ instead of $\frac{f_d}{g_d}$ from Eq. (11) to Eq. (26), the formula of a Λ-shaped 3-level system can be obtained. Table 2 lists the parameters for 1064 nm laser.

Table 2. The π-polarization parameters of Nd:YVO_4 at T=300 K

Wavelength (nm)	808	880	888	914
f_a/g_a	0.4007	0.4007	0.2387	0.0502
f_d/g_d	0.0036	0.5110	0.5110	0.5110
f_b/g_b	0.5110	0.5110	0.5110	0.5110
f_c/g_c(×10^{-5})	3.22	3.22	3.22	3.22
$\sigma_{ab}(f_a/g_a)$(×10^{-21}cm^2)	321	108	9.5	4.12
τ_0 (μs)	91	91	91	91
$I_{PS}(0)$ (W/cm^2)	748	909	7348	4654

The listed parameters on Table 2 are obtained by measuring a 0.27% Nd doped YVO_4 crystal, where the number density of Nd^{3+} ions is related to $N_{Nd:YVO_4,1\%} = 1.37 \times 10^{20}$(cm^{-3}) (Notes: In some references, the atomic density of Nd:YVO_4 is 1.26×10^{20}cm^{-3}). Based on the parameters, the population distributions in the manifold of $^4F_{3/2}$ are calculated and shown in Fig. 5, when an identical pump power density of 5 kW/cm^2 at different wavelengths (808, 880, 888, and 914 nm) is applied on Nd:YVO_4 crystal.

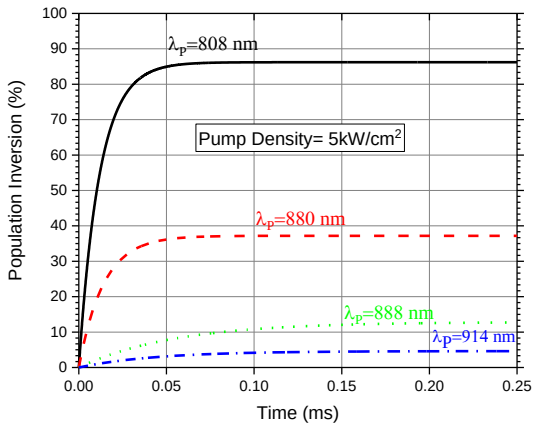

Fig. 5. Population inversion of 1064nm Nd:YVO_4 laser when a 5 kW/cm^2 pump power density is applied on the crystal at T=300 K.

The σ-polarization performances of Nd:YVO_4 lasers, like 1066 nm laser, can be simulated in a similar method. For other Nd^{3+} doped laser crystals, such as Nd:YAG, the corresponding results can be obtained by choosing appropriate parameters. These results will be meaningful for the investigation of in-band pumped CW Nd:YAG NPRO, the heart of large-scale laser interferometer (the important tool in the search of .gravitational waves and others). Eq. (16) and Eq. (24) show other important consequence that the effective upper-state lifetime is a function of pump and laser intensities and their saturations. The application includes the research of passively mode-locked laser with saturable absorber, especially mode-locking with slow absorber.

The excellent CW performances of in-band pumped Nd:YVO_4 laser have been demonstrated, where 880, 888, and 914 nm diode were used a pump source over the 808 nm one. However, the Q-switched and pulse amplified performances of in-band pumped laser were disappointing. In my analysis, the laser system is regarded as two thermodynamic equilibrium systems, upper state and lower state. The pump absorption/saturation are functions of laser intensity within the medium, and conversely the laser gain/saturation are functions of

pump intensity within the medium, and even the effective upper state lifetime is a function of pump and laser intensities and their saturations. In-band pumping has lower population inversion limitation than off-band pumping. No fabricated parameters are needed for the numerical simulation. The results are very close to experimental ones.

Acknowledgment. This work was supported by NASA Goddard Space Flight Center IRAD fund. The author thanks Drs. Michael Krainak, Anthony Yu, and Steven Li (NASA GSFC) for their valuable discussions, and acknowledges the spectral measurement of Nd:YVO_4 crystal completed by Robin Bai (a UVA student and NASA scholarship winner) and Dr. Songsheng Chen (NASA Langley Research Center). The paper partially includes Robin's consequences in his investigation of in-band direct pumped Nd:YAG NPRO.

References:

1. R. Newman, J. Appl. Phys. Vol.34, 437 (1963). https://doi.org/10.1063/1.1702627
2. K. Contag, M. Karszewski, C. Stewen, A. Giesen, and H. Hugel, Quantum Electronics 29 (8) 697-703 (1999). doi:10.1070/QE1999v029n08ABEH001555
3. C. R. Giles, C. A. Bums, D. J. DiGiovanni, N. K. Dutta, and G. Raybon, IEEE PHOTONICS TECHNOLOGY LETTERS, VOL. 3, 363 (1991).**DOI:** 10.1109/68.82113
4. Alex Dergachev, Peter F. Moulton, and Thomas E. Drake, Advanced Solid-State Photonics (TOPS), OSA Trends in Optics and Photonics, 608 (2005) •https://doi.org/10.1364/ASSP.2005.608
5. Z. Huang, Y. Huang, Y. Chen, and Z. Luo, J. Opt. Soc. Am. B 22, 2564–2569 (2005). •https://doi.org/10.1364/JOSAB.22.002564
6. Marwan Abdou Ahmed, Matthias Haefner, Moritz Vogel, Christof Pruss, Andreas Voss, Wolfgang Osten, and Thomas Graf, Optics Express, Vol. 19, 5093-5103 (2011). •https://doi.org/10.1364/OE.19.005093
7. Y. Jeong, J.K. Sahu, D. N. Payne, and J. Nilsson, Optics Express, Vol. 12, 6088-6092 (2004). •https://doi.org/10.1364/OPEX.12.006088
8. L. McDonagh, R. Wallenstein, R. Knappe, and A. Nebel, Opt. Lett. 31, 3297–3299 (2006).https://doi.org/10.1364/OL.31.003297
9. Weiping Deng, Tao Yang, Jianping Cao, Erjun Zang, Liufeng Li, Lisheng Chen, and Zhanjun Fang, Opt. Lett. 43, 1562–1565 (2018). https://doi.org/10.1364/OL.43.001562D.
10. Sangla, M. Castaing, F. Balembois, and P. Georges, Opt. Lett. 34, 2159–2161 (2009). •https://doi.org/10.1364/OL.34.002159
11. S. Li, A Yu, M. Krainak, Y. Bai, O. Konoplev, M. Fahey, and K. Numata, Solid State Laser XXVII: Technology and devices, Proceedings of SPIE, Vol.10511, (2018). https://doi.org/10.1117/12.2290419
12. Xavier Délen, François Balembois, Olivier Musset, Patrick Georges, J. Opt. Soc. Am. B 28, 52-57 (2010). https://doi.org/10.1364/JOSAB.28.000052
13. The energy level diagram was elaborated based on the values on the following reference: A. A. Kaminskii, "Crystalline Lasers: Physical Processes and Optical Schemes," (CRC Press, Inc., 1996), pp.137.1
14. A. Schlatter, L. Krainer, M. Golling, R. Paschotta, D. Ebling, and U. YVO_4 laser," Opt. Lett. 30, 44-46 (2005). •https://doi.org/10.1364/OL.30.000044